Applied Surface Science 476 (2019) 128–135

Contents lists available at ScienceDirect

Applied Surface Science

journal homepage: www.elsevier.com/locate/apsusc

Full Length Article

Fabrication and characterization of diffraction gratings in ophthalmic polymers by using UV direct laser interference patterning

D. Sola[a,*], S. Alamri[b], A.F. Lasagni[b,c], P. Artal[a]

[a] Laboratorio de Óptica, Centro de Investigación en Óptica y Nanofísica, Universidad de Murcia, Campus Espinardo, 30100 Murcia, Spain
[b] Fraunhofer-Institut für Werkstoff- und Strahltechnik IWS, Winterbergstr. 28, 01277 Dresden, Germany
[c] Institut für Fertigungstechnik, Technische Universität Dresden, Zeunerbau, George-Bähr-Str. 3c, 01062 Dresden, Germany

ARTICLE INFO

Keywords:
Direct laser interference patterning
Laser materials processing
Surface structuring
Polymers
Diffraction gratings

ABSTRACT

The fabrication of diffractive elements in ophthalmic polymers to induce refractive index changes which may be applied for refractive correction is of great interest in the fields of Optics and Ophthalmology. In this work, polyhydroxyethyl-methacrylate and silicone hydrogel polymers used as soft contact lenses were structured with linear periodic patterns by means of Direct Laser Interference Patterning (DLIP). As the laser source, a Q-switched laser system emitting 10 ns pulses at a wavelength of 266 nm was used to generate the periodic modulation on the surface of the polymer materials. The experiments were carried out employing a two-beam interference setup, studying the features of the laser processed areas as a function of both the laser fluence and the interference period. The topography of the structured areas was investigated using optical confocal microscopy. Compositional and structural modifications on the materials were studied by means of micro-Raman spectroscopy, scanning electron microscopy (SEM) and energy dispersive X-ray spectroscopy (EDX). Finally, periodic patterns were characterized through diffractive techniques under illumination of a continuous-wave 632.8 nm He-Ne laser to determine the diffractive properties of the DLIP periodic patterns and the refractive index change induced by the laser processing.

1. Introduction

Nowadays the modification of the refractive power of the eye to correct visual refractive errors is carried out by laser refractive surgery. Among the techniques commonly used, the most noteworthy are laser in situ keratomileusis, LASIK, and photorefractive keratectomy, PRK [1–3]. These techniques use UV laser radiation to reshape the cornea through photo-ablative decomposition processes, resulting destructive, invasive and irreversible. In addition, these procedures may entail postsurgical complications and secondary visual effects such as dry eye, stromal haze, irregular astigmatism and keratoconus [4–6].

Short and ultrashort laser pulses have been widely applied to fabricate two- and three-dimensional permanent structures inside transparent optical materials such as waveguides, photonic crystals, diffraction gratings, and beam splitters [7–15]. During the last decade ultrafast laser inscription, ULI, has been proposed as a new approach to change the power of refractive optical elements for ophthalmic applications. In particular, linear diffraction gratings were inscribed within dye-doped and non-doped ophthalmic polymers, ex-vivo and in-vivo corneal stroma by using high-repetition-rate ultrashort laser pulses with pulse energy below damage threshold. Refractive index modification achieved ranged 6×10^{-2}–8×10^{-2} in polymers and 2.1×10^{-2}–3.7×10^{-2} in ocular tissues [16–23]. Nevertheless, the time required to process areas of similar dimensions to that of the cornea, even at the maximal scanning speed reported to date, 15 mm/s [21], is too long and makes this technique inviable to be applied at real scale.

This technological limitation may be overcome by using direct laser interference patterning, DLIP. This single-step and non-contact laser processing technique has been used to fabricate periodic arrays in a wide range of metals and polymers [24–33]. DLIP consists in the interference of two or more pulsed laser beams to generate a spatial variation of intensity which is transferred to the substrate to create periodic patterns with controlled dimensions and whose geometry is managed by the interference angle, the laser wavelength and the partial laser intensity. This technique has been demonstrated to be more flexible and cost-effective when compared to traditional micro- and sub-micrometre structuring methods, can be easily implemented in manufacturing processes at industrial level and can be applied to produce periodic patterns on macroscopic areas in very short times. It is

* Corresponding author.
E-mail address: daniel.sola@um.es (D. Sola).

https://doi.org/10.1016/j.apsusc.2019.01.071
Received 28 August 2018; Received in revised form 13 December 2018; Accepted 8 January 2019
Available online 09 January 2019
0169-4332/

worth highlighting that to date the maximal processing rate achieved in polymers is 0.9 m^2/min [31].

The assessment of this laser processing technique to be used for refractive correction requires, as a first approach, a thorough investigation in ophthalmic polymers prior to be used in ex-vivo or in-vivo ocular tissues. In this framework, we previously reported on the fabrication of diffraction gratings in polydimethylsiloxane, PDMS, intraocular lenses [34]. Results achieved in this material were very remarkable, obtaining refractive index changes one order of magnitude higher than those reported by using the ULI technique.

In this work we report on the fabrication and characterization of diffractive gratings in poly-hydroxyethyl-methacrylate and silicone hydrogel polymers used as soft contact lenses by using direct laser interference patterning, DLIP. These materials are particularly interesting since they are hydrophilic, and the processing results might depend not only on the laser working parameters but also on the hydration stage. Therefore, we process for the first-time ophthalmic polymers sensitive to hydration stage by using DLIP. This study will provide us a background for tackling the processing of ocular tissues, whose properties also depend on the hydration stage. In particular, in this work we have processed the samples in dry stage. Diffraction gratings were structured by means of a pulsed laser emitting at 266 nm with pulsewidth in the nanosecond range. The surface topography of the irradiated areas was investigated using optical confocal microscopy, bright filed and phase contrast microscopy, and Scanning Electron Microscopy, SEM. Also, compositional and structural modification was studied by means of Energy Dispersive X-ray Spectroscopy, EDX, and micro-Raman spectroscopy. Finally, periodic patterns were characterized by diffractive techniques to ascertain the diffractive properties of the DLIP periodic patterns.

2. Experimental

2.1. Laser processing

A Q-Switched Nd:YAG laser emitting 10 ns pulses at a wavelength of 266 nm with a repetition rate of 10 Hz was used as the laser source to fabricate the periodic structures (Quanta Ray, Spectra Physics). Laser processing was carried out under the two-beam configuration, as shown in Fig. 1, so that the laser beam was split into two beams of equal intensity by a beam splitter and the optical path of both beams was adjusted by mirrors and lenses. The interference period, Λ, was controlled by the angle between the laser beams, 2α, and the laser wavelength, λ, of the laser light according to the following equation [27]:

$$\Lambda = \frac{\lambda}{2 \sin \alpha} \quad (1)$$

Experiments were carried out setting interference periods at 2.6 μm and 4.7 μm. Features of the laser processed areas were also studied as a function of the laser fluence, delivering fluences on the surface of the samples between 0.5 J/cm^2 and 17 J/cm^2, and number of pulses, between 1 and 5 pulses. To structure large areas, a 0.5 mm side square mask was used to obtain a square pixel and the sample was translated in x and y directions controlling the distance between adjacent pixels. Since the mask was located at a significant distance from the laser source, the shape of the beam at this position can be considered Gaussian. Then, two 100 mm optical lenses were used to focus the interference pattern on the surface of the sample, as shown in Fig. 1 (double lens system).

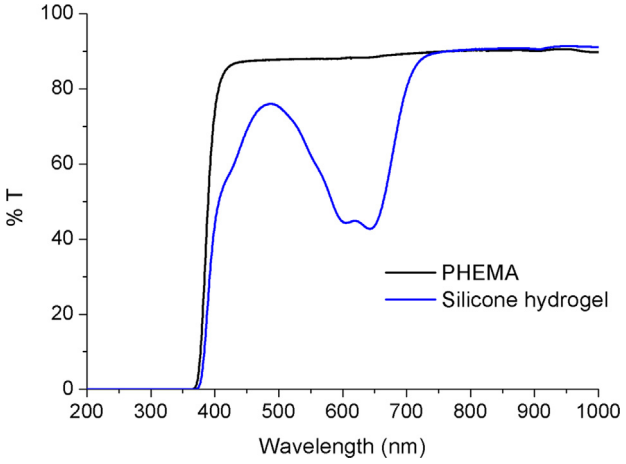

Fig. 2. Transmission spectra of both polymer samples.

2.2. Materials

Polymacon (poly-hydroxyethyl-methacrylate, PHEMA) and Safrofilcon A (silicone hydrogel) both manufactured by Contamac were used as substrates. These polymers are commonly used as soft contact lenses. The samples were 1 mm thick and were processed in dry stage. Fig. 2 shows the transmission spectra of both samples and Table 1 presents the main physical properties.

2.3. Characterization techniques

Superficial topography and profile measurements were carried out using an optical confocal microscope (Sensofar S Neox). Bright field and phase contrast images were taken using a phase contrast microscope (M-800, Optika). Microstructural and semi-quantitative compositional analyses were determined by environmental Field Emission Gun Scanning Electron Microscopy, FEG-SEM, (Quanta FEG-250) with Energy Dispersive X-ray Spectroscopy, EDX, detector incorporated. It should be noted that EDX technique allows the determination of most elements present in concentration above 0.1% with an estimated accuracy of ± 5%. Micro-Raman dispersion measurements were performed using a spectrograph (SR-303i-B, Andor) equipped with a thermoelectric-cooled CCD detector (DU920P-BEX2-DD, Andor). As the excitation source, a 532 nm laser was used, and the scattered light was collected in confocal configuration through a 60× (NA = 0.85)

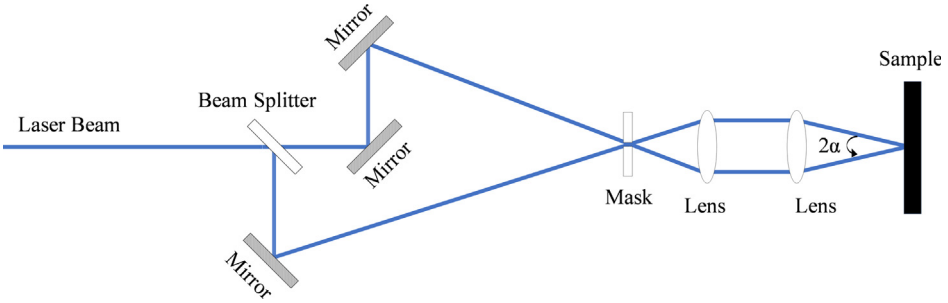

Fig. 1. Schematic representation of the DLIP two-beam interference configuration setup.

Table 1
Physical properties of Polymacon (PHEMA) and Safrofilcon A (silicone hydrogel).

Property	Polymacon[a]	Safrofilcon A[a]
Density (g/cm^3)	1.27	1.10
Oxygen permeability at 35 °C (barrers)	7.9	62
Water content at 20 °C by weight (%)	40	65
Swell factor at 20 °C	1.20	1.45
Refractive index at 20 °C dry	1.510	1.485
Refractive index at 20 °C hydrated	1.438	1.385
Melting point (°C)	155.9	132.3
Shore D hardness	88	83
Tensile strength (MPa)	0.44	1

[a] Data provided by the manufacturer, Contamac.

microscope objective lens. The output power of the laser was kept below 25 mW in order to avoid significant local heating of the samples. A continuous-wave 3 mW He-Ne laser at 632.8 nm was used to illuminate the DLIP periodic patterns to characterize the diffractive modes.

3. Results and discussion

3.1. Direct laser interference patterning

Periodic line-like patterns arrays were produced on the polymer samples using a two-beam laser interference setup, for which the modulation of the intensity profile experienced on the surface of the sample can be described according to the equation [27]:

$$I_P(x, y) = 4 I_L \cos^2\left(\frac{2\pi}{\lambda} x \sin\alpha\right) \quad (2)$$

where x and y are the coordinate axes in the perpendicular and parallel directions to the linear pattern respectively, I_L is the laser fluence of each beam, 2α the interference angle and λ the laser wavelength. This distribution of intensity may be transferred onto the material surface by photo-thermal, photo-chemical or photo-physical processes. Considering the high absorption of the polymer samples at the laser wavelength used to carry out the process, 266 nm, and that the pulse duration is in the nanosecond range, 10 ns, both photo-chemical and photo-thermal processes will take part in the structuring process implying direct bond breaking and thermally induced vaporization processes [35].

The experimental setup was adjusted according to the Eq. (1) to structure both types of polymer samples with spatial periods of 2.6 μm and 4.7 μm. Single-pulse laser structuring was assessed modifying the laser fluence between 0.5 J/cm^2 and 3.5 J/cm^2 for the silicone hydrogel and between 7 J/cm^2 and 17 J/cm^2 for the PHEMA sample. Multi-pulse laser structuring was investigated in the PHEMA sample, delivering 1, 3 and 5 pulses at a fluence of 17 J/cm^2. As an example, Fig. 3 shows surface topographies of a PHEMA sample structured with a period Λ of 2.6 μm obtained using one laser pulse and a laser fluence of 7 J/cm^2, and a silicone hydrogel structured with a period of 4.7 μm using a single laser pulse and a laser fluence of 1.6 J/cm^2, (a) and (b) respectively. Profile measurements carried out in the processed areas by confocal microscopy allowed determining the experimental period of the interference pattern, resulting in 2.64 ± 0.15 μm and 4.78 ± 0.48 μm, in good agreement with the theoretical calculation provided by Eq. (1). At low laser fluences it was observed that laser-matter interaction process in both polymers resulted in the swelling of the polymer surface, as shown in Fig. 4 in which a confocal topography (a) and a profile (b) of the swelling obtained in the PHEMA polymer processed with a single pulse at a laser fluence of 0.37 J/cm^2 is presented. Swelling is a pre-ablative process commonly observed at low fluences, which consists in the softening of the irradiated surface giving rise to the material expansion. This process has been observed under certain conditions and may be attributed to both a local heating of the polymer sample and the

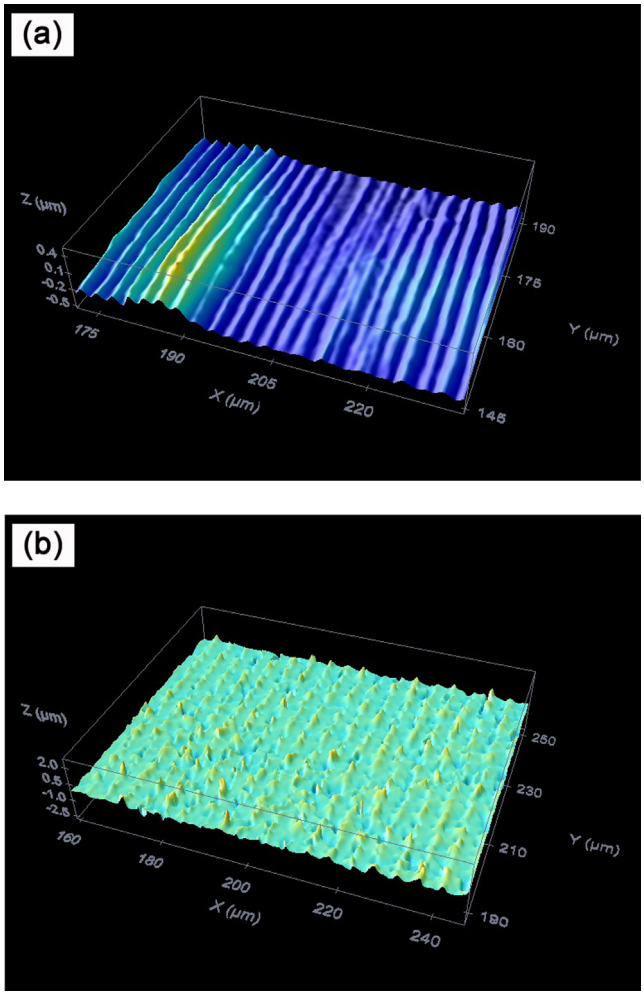

Fig. 3. Confocal images of a PHEMA sample structured with a period of 2.6 μm obtained using one laser pulse and a laser fluence of 7 J/cm^2 (a), and a silicone hydrogel structured with a period of 4.7 μm using a single laser pulse and a laser fluence of 1.6 J/cm^2 (b).

decomposition of the UV absorbers of the polymer sample, which results in molecular nitrogen elimination and eventually to other gaseous byproducts [32,35–38].

It was observed that the height of DLIP structures increased with the laser fluence in both single-pulse and multi-pulse modes, as shown in Fig. 5. In addition, as previously reported, the height of the periodic structure decreased when the spatial period was decreased from 4.7 μm to 2.6 μm [32]. It is worth mentioning that the optimal fluence required to structure the silicone hydrogel polymer was much lower than in the case of the PHEMA sample which may be related to the difference in the mechanical properties of each polymer. It has been reported that in ceramics, glass-ceramics and glasses the ablation efficiency strongly depends on the mechanical properties so that the harder the material the lower the ablation efficiency [39–41]. In this case, the hardness of the silicone hydrogel is lower than for the PHEMA polymer. As an example, for a spatial period of 4.7 μm to achieve a structured height of 0.6 μm requires a delivered fluence of around 1 J/cm^2 for the silicone hydrogel whereas for the PHEMA 17 J/cm^2 are required, as shown in Fig. 5.

Nevertheless, it was observed that high fluences achieved at both single and multi-pulse modes induced a heat affected zone, HAZ, in the processed areas as a consequence of the photothermal-mechanical nature of the laser-matter interaction process. In this type of laser ablation, a thin layer of material in liquid-phase is formed in the interaction zone and the recoil pressure produced in the process squeezes the

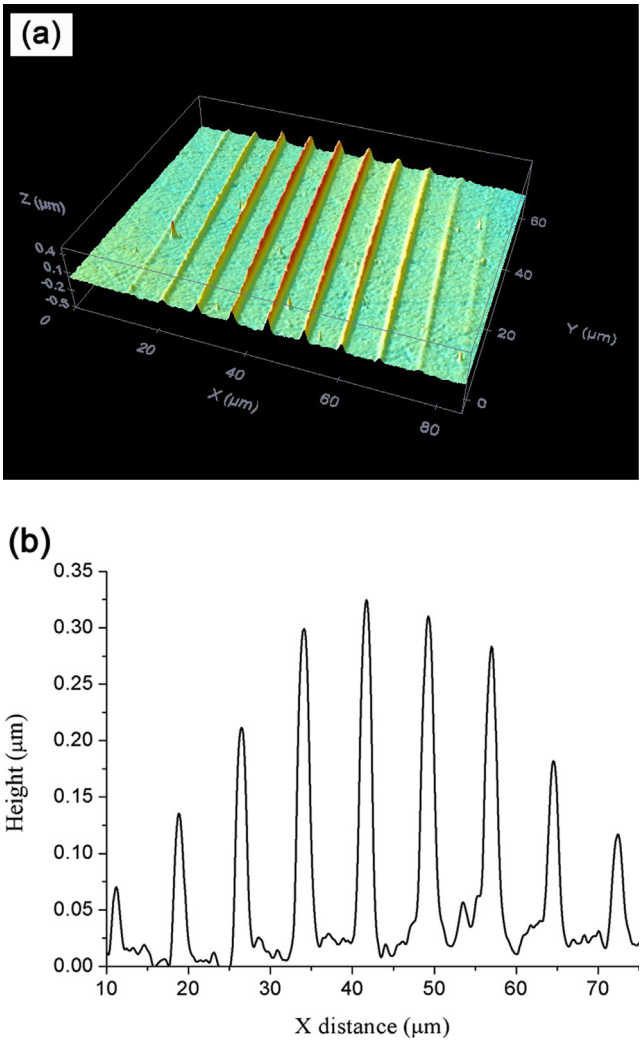

Fig. 4. Confocal topography (a) and profile (b) of swelling phenomenon in the PHEMA sample processed with a single pulse at a laser fluence of 0.37 J/cm^2.

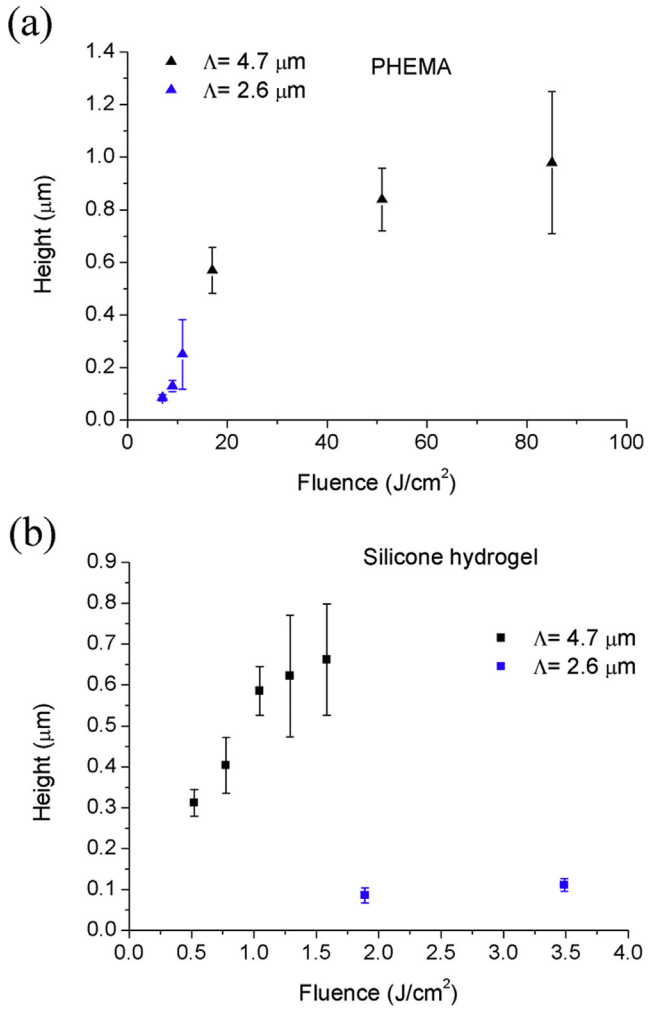

Fig. 5. Height of DLIP structures as a function of delivered fluence. PHEMA sample with a structuring period Λ = 2.6 μm was processed increasing laser fluence between 7.0 J/cm^2 and 11.5 J/cm^2 in single-pulse mode and sample with a structuring period Λ = 4.7 μm using 1, 3 and 5 laser pulses using a laser fluence of 17 J/cm^2 (a). Silicone hydrogel was processed using single-pulse mode increasing laser fluence between 0.5 J/cm^2 and 3.5 J/cm^2 (b).

liquid out from the interaction zone and the material is removed from the surface via evaporation and liquid-phase expulsion [40,42]. As an example, Fig. 6 shows a top-view SEM micrograph of a PHEMA sample processed with a single pulse at a fluence of 11 J/cm^2 and a spatial period of 2.6 μm in which the molten material produced during the ablation process and redeposited on the interaction zone is observed.

3.2. Microstructural and compositional characterization

Processed areas were characterized by EDX to analyze the effects caused in the polymers as consequence of DLIP structuring. Tables 2 and 3 show the main elements the polymers were made up of as well as the elements found in the processed areas. Semi-quantitative compositional analyses showed that in both polymer samples the increase in the laser fluence gave rise to an increase in the carbon content. In addition, in the silicone hydrogel there was a decrease in the most volatile elements, nitrogen and fluorine. Therefore, under high-fluence experimental conditions the polymer underwent degradation in the laser-treated areas as a consequence of the photo-thermal nature of the laser interaction process.

Chemical composition and structural analyses of the laser treated polymers were also investigated by μ-Raman spectroscopy. Fig. 7 shows Raman spectra of both polymers in non-processed areas and in the DLIP structured regions at both low and high laser fluences. Raman spectra were made up of sharp peaks and broad bands which in the case of the PHEMA sample can be assigned as follows [43,44]: 473 cm^{-1}, deformation mode; 604 cm^{-1}, ν_sCCO; 830 cm^{-1}, ν_sCOC; 897 cm^{-1}, ν_sCOC(H); 968 cm^{-1}, ρCH$_3$; 1029 cm^{-1}, νCC; 1089 cm^{-1}, ν_{as}OCH$_2$C, ρCH$_3$, and ρCH$_2$; 1204 cm^{-1}, τCH$_2$ and ωCH$_2$; 1277 cm^{-1}, τCH$_2$ and ωCH$_2$; 1455 cm^{-1}, δCH$_2$ and δCH$_3$; and 1718 cm^{-1}, νC=O. Concerning the silicone hydrogel the main bands and peaks assignment is [45,46]: 601 cm^{-1}, ν_sCCO; 637 cm^{-1}, SiO$_3$; 761 cm^{-1}, SiCH$_3$; 1111 cm^{-1}, νCC; 1411 cm^{-1}, δCH$_2$; 1449 cm^{-1} δCH$_2$ and δCH$_3$; 1628 cm^{-1} νCO.

Raman spectra of DLIP structured areas processed at high fluence showed significant variations when compared to that corresponding to the non-processed samples. In particular, in the PHEMA sample processed at high laser fluence there was a strong decrease of the peak intensity in the components at 473 cm^{-1}, 604 cm^{-1}, 830 cm^{-1}, 897 cm^{-1}, 1089 cm^{-1} and 1718 cm^{-1}, whereas the components at 734 cm^{-1}, 1204 cm^{-1}, 1230 cm^{-1} disappeared. In the silicone hydrogel processed at high laser fluence the peak intensity of the components at 761 cm^{-1}, 1449 cm^{-1} and 1628 cm^{-1} decreased substantially and the component at 601 cm^{-1} turned into a shoulder of the peak at 637 cm^{-1}. Conversely, at low fluence the laser structuring was not accompanied with important changes in the Raman spectra and hence the polymer structure remained almost unaltered after laser irradiation. Mechanisms responsible for refractive index changes are not

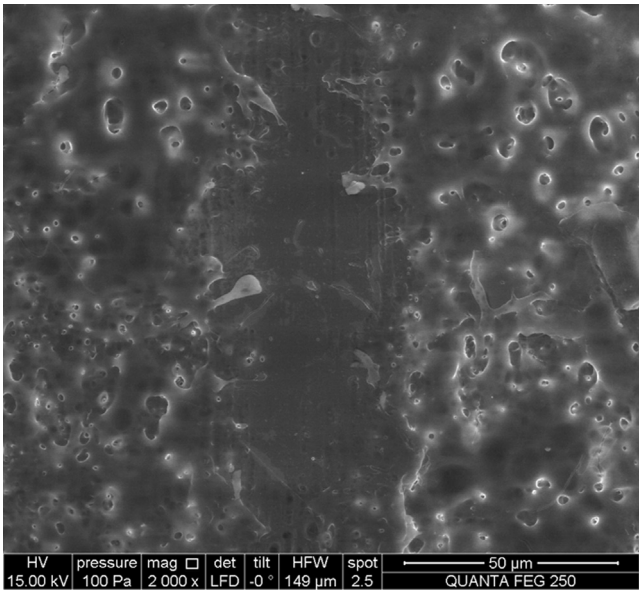

Fig. 6. Top-view SEM micrograph of a PHEMA sample processed with a single pulse at a fluence of 11 J/cm^2 and a spatial period of 2.6 µm.

Table 2
Compositional analysis in at% of PHEMA and laser processed areas measured by EDX.

	C	O
Non-processed	70.81	29.19
7.0 J/cm^2	73.73	26.27
9.4 J/cm^2	73.56	26.44
11.0 J/cm^2	74.03	25.97
11.5 J/cm^2	74.21	25.79
HAZ	74.25	25.75

Table 3
Compositional analysis in at% of silicone hydrogel and laser processed areas measured by EDX.

	C	N	O	F	Al	Si
Non-processed	70.85	6.73	14.80	2.24	0.09	5.29
1.9 J/cm^2	71.53	6.59	14.37	1.97	0.21	5.33
3.5 J/cm^2	72.73	5.42	14.10	1.88	0.44	5.43

yet clear and they may be attributed to photodecomposition, local heat accumulation, dehydration, additional cross-linking and tensile stress [46–49]. The strong fluorescence background increase observed in samples processed at high fluence can be assigned to thermal decomposition of organic molecules [46]. On the other hand, when laser processed areas do not present significant changes in the structure of the polymer matrix, such as samples processed at low laser fluence, the refractive index mechanism can be attributed to additional cross-linking and local densification [46].

3.3. Optical characterization

In order to evaluate the refractive index changes achieved in the DLIP periodic patterns structured on the polymer samples, processed areas were characterized under illumination of a continuous-wave He-Ne laser at 632.8 nm. DLIP periodic patterns showed diffraction patterns at both spatial periods, 4.7 µm and 2.6 µm with diffraction angles in good agreement with the diffraction equation $m\lambda = \Lambda \sin\theta$, where m is the diffraction order, λ the laser wavelength and Λ the grating period. As an example, Fig. 8 shows far-field diffraction patterns obtained from

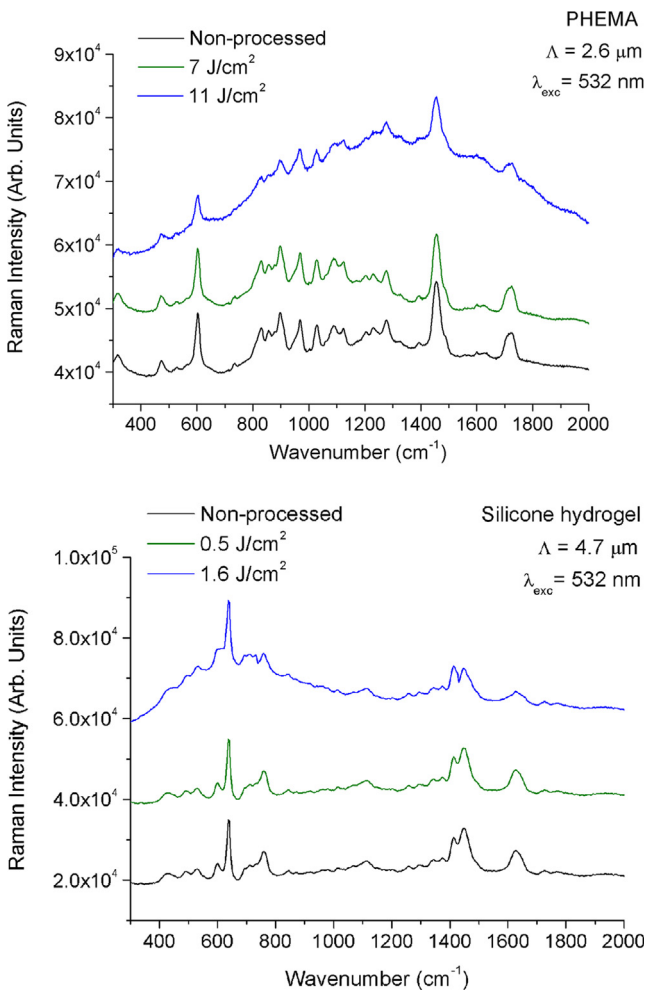

Fig. 7. Micro-Raman spectra of PHEMA and silicone hydrogel samples.

single-pulse mode processed samples, 8(a) corresponding to a PHEMA sample processed at a fluence of 17 J/cm^2 and a structuring period Λ = 4.7 µm, and 8(b) to a silicone hydrogel sample processed with 1.9 J/cm^2 and a structuring period Λ = 2.6 µm. Next, the intensity of each diffracted order was measured by using a power-meter and the first-order, the second-order and the total efficiency was evaluated. As shown in Fig. 9, both first- and second-order efficiencies augmented as the laser fluence increased as in single-pulse as in multi-pulse mode. In the PHEMA sample these efficiencies were higher for the case of multi-pulse mode. Also, it is worth mentioning that first-order efficiency followed a linear trend for both samples, pointing out that non-linear multi-photon absorption processes were not involved in the DLIP structuring process [47]. Tables 4 and 5 show total efficiency as a function of the delivered laser fluence for both samples. It is worthy of highlight that only samples processed with a spatial period of Λ = 4.7 µm at the lowest laser fluences, 14.0 J/cm^2 and 17 J/cm^2 for the PHEMA, and 0.5 J/cm^2 and 0.8 J/cm^2 for the silicone hydrogel, achieved a total efficiency equal of higher than 98%, whereas the highest diffraction efficiencies obtained for Λ = 2.6 µm were 0.963 and 0.958 for PHEMA and silicon hydrogel respectively. Diffraction gratings with efficiencies equal or higher than 98% were very difficult to be observed in bright field microscopy and could only be assessed in phase contrast mode, as shown in Fig. 10, in which bright field (a) and phase contrast (b) images of a DLIP processed sample at a laser fluence of 17 J/cm^2 and a spatial period of Λ = 4.7 µm are shown, indicating that these structures exhibited very low scattering loss. Therefore, refractive index change assessment was only carried out in PHEMA and silicone hydrogel samples processed with a spatial period of Λ = 4.7 µm and

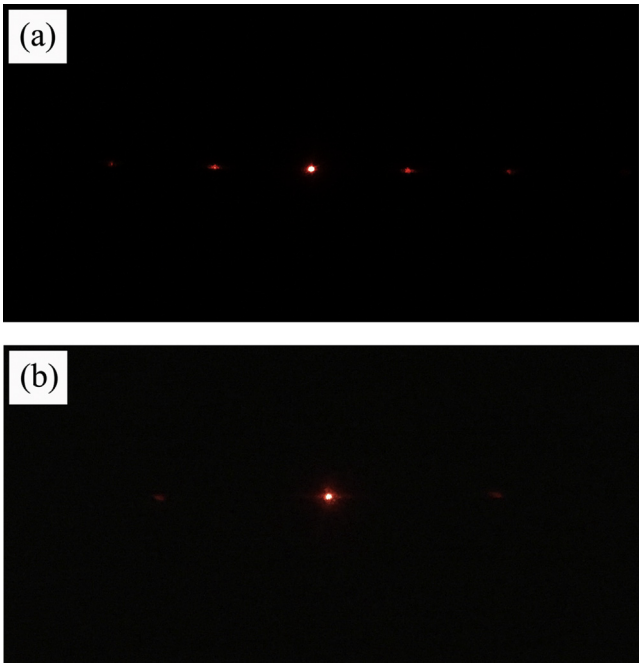

Fig. 8. Diffraction images of DLIP periodic patterns obtained in single-pulse mode from a PHEMA sample at a fluence of 17 J/cm^2 and a structuring period Λ = 4.7 μm (a), and from a silicone hydrogel sample processed with 1.9 J/cm^2 and a structuring period Λ = 2.6 μm (b).

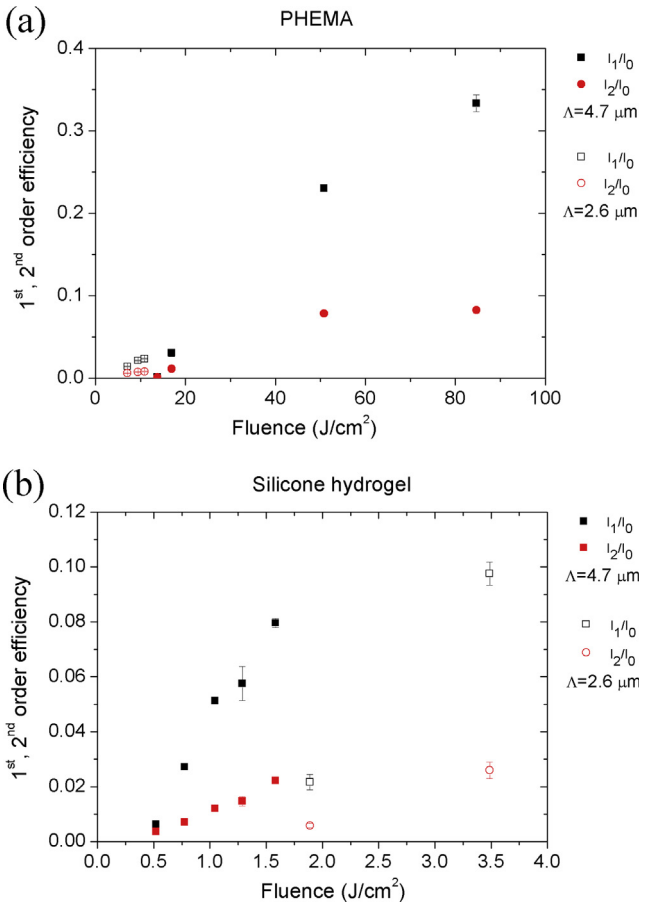

Fig. 9. First and second-order efficiency of both PHEMA (a) and silicone hydrogel (b) samples as a function of the delivered fluence.

Table 4
Efficiency and refractive index modification for the PHEMA samples.

Λ (μm)	F (J/cm^2)	Efficiency	Δn
4.7	14.0	0.980 ± 0.017	7.80×10^{-2}
4.7	17.0	0.983 ± 0.017	5.60×10^{-2}
4.7	51.0	0.743 ± 0.021	–
4.7	85.0	0.284 ± 0.007	–
2.6	7.0	0.963 ± 0.005	–
2.6	9.4	0.831 ± 0.016	–
2.6	11.0	0.517 ± 0.027	–

Table 5
Efficiency and refractive index modification for the silicone hydrogel samples.

Λ (μm)	F (J/cm^2)	Efficiency	Δn
4.7	0.5	0.989 ± 0.007	5.30×10^{-2}
4.7	0.8	0.981 ± 0.008	8.50×10^{-2}
4.7	1.0	0.896 ± 0.010	–
4.7	1.3	0.742 ± 0.033	–
4.7	1.6	0.632 ± 0.027	–
2.6	1.9	0.958 ± 0.026	–
2.6	3.5	0.332 ± 0.032	–

laser fluences of 14.0 J/cm^2 and 17 J/cm^2 for the PHEMA, and 0.5 J/cm^2 and 0.8 J/cm^2 for the silicone hydrogel, which were considered the optimal processing conditions. Moreover, as shown in the previous section, samples structured with these processing conditions did not present significant changes when compared to non-processed samples.

Refractive index change, under the former considerations, can be calculated considering the diffraction grating as a phase grating in which the refractive index change was both uniform and top-hat shaped within the irradiated region. With these assumptions the intensity of the 0th and 1st order diffracted light can be expressed as [16]:

$$I_0 = \left(\frac{1}{\lambda z}\right)^2 \left[\left(e^{i2\pi\frac{(n+\Delta n)b}{\lambda}} - e^{i2\pi\frac{nb}{\lambda}}\right)\frac{a}{\Lambda} + e^{i2\pi\frac{nb}{\lambda}}\right]^2 \quad (3)$$

and

$$I_1 = \left(\frac{1}{\lambda z}\right)^2 \left[\left(e^{i2\pi\frac{(n+\Delta n)b}{\lambda}} - e^{i2\pi\frac{nb}{\lambda}}\right)\frac{a}{\Lambda}\mathrm{sinc}\left(\frac{a}{\Lambda}\right)\right]^2 \quad (4)$$

where λ is the laser wavelength, n the refractive index of the material, b the thickness of the grating line, a the width of the grating line and Λ the grating period. Next, the first-order efficiency provided by the ratio of Eqs. (4) and (3) was plotted versus the refractive index change, Δn. Taking into account the first-order efficiency for the optimal processing conditions, 0.0013 and 0.0307 for the PHEMA at 14.0 J/cm^2 and 17 J/cm^2 respectively, and 0.0062 and 0.0272 for the silicone hydrogel at 0.5 J/cm^2 and 0.8 J/cm^2 respectively, the corresponding refractive index changes were found to be 7.8×10^{-2} and 5.6×10^{-2} for the PHEMA at 14 J/cm^2 and 17 J/cm^2 respectively, and 5.3×10^{-2} and 8.5×10^{-2} for the silicone hydrogel at 0.5 J/cm^2 and 0.8 J/cm^2, Tables 4 and 5. The refractive index modification obtained in the DLIP structured polymers was slightly higher to those previously reported by using the ULI technique in silicone and non-silicone based hydrogel polymers 6×10^{-2} [16], and in the same order of magnitude in dye-doped silicone hydrogels 8×10^{-2} [18]. It is worth highlighting that these gratings were manufactured at 0.4 μm/s and 600 μm/s for the non-doped and doped polymers respectively so that the fabrication yields for a grating with a spatial period of 4.7 μm would be 1.88×10^{-6} mm^2/s and 2.82×10^{-3} mm^2/s respectively, whereas the fabrication yield for the same grating manufactured by DLIP in the experimental conditions studied in this work ranges 0.23 mm^2/s and 2.2 mm^2/s, more than two orders of magnitude faster.

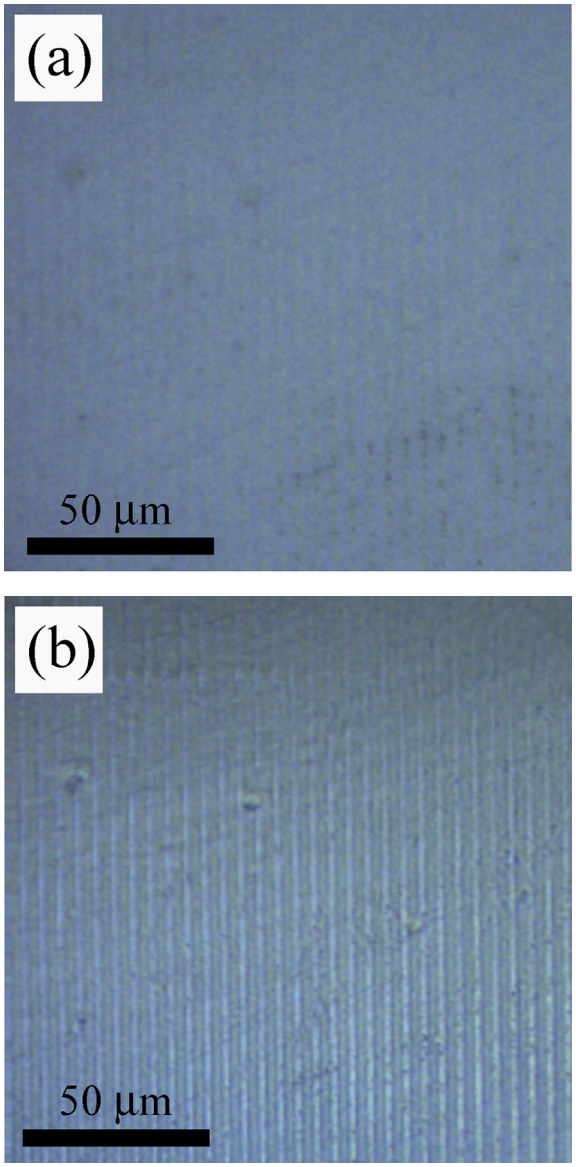

Fig. 10. Bright field (a) and phase contrast (b) images of DLIP structured PHEMA at a laser fluence of 17 J/cm^2 and a spatial period of $\Lambda = 4.7$ μm.

4. Conclusions

Direct laser interference patterning was successfully applied to structure PHEMA and silicone hydrogel polymers used as soft contact lenses. A Q-switched laser delivering 10 ns laser pulses at 266 nm and the two-beam configuration setup were used to fabricate periodic line-like patterns with spatial periods of 2.6 μm and 4.7 μm. At low laser fluences it was observed that laser-matter interaction process in both polymers resulted in the swelling of the polymer surface. As the laser fluence increased the height of the DLIP structure also increased in both single-pulse and multi-pulse processing modes. Furthermore, the height of the periodic structure decreased when decreasing the spatial period. However, high laser fluences achieved at both single and multi-pulse modes induced a heat affected zone in which the material removed from the surface during the laser interaction process was redeposited on the interaction zone. SEM-EDX and micro-Raman analyses carried out in the processed areas showed that at low laser fluence the material remained almost unaltered. On the contrary, at high laser fluence the material underwent degradation with significant changes in the chemical structure showing a strong fluorescence background attributed to thermal decomposition of organic molecules. DLIP structured areas showed diffraction patterns at both spatial periods, 4.7 μm and 2.6 μm. Assessment of first- and second-order efficiency showed that they augmented with the laser fluence increase as in single-pulse as in multi-pulse processing mode. Nevertheless, total diffraction efficiency decreased with the laser fluence increase. Moreover, only samples processed with a spatial period of $\Lambda = 4.7$ μm at the lowest laser fluences, 14.0 J/cm^2 and 17 J/cm^2 for the PHEMA, and 0.5 J/cm^2 and 0.8 J/cm^2 for the silicone hydrogel, achieved a total efficiency equal of higher than 98%, thus determining these processing parameters as the optimal processing conditions. 1st to 0th order diffracted light efficiency was used to assess the refractive index modification, resulting in 7.8×10^{-2} and 5.6×10^{-2} for the PHEMA at 14 J/cm^2 and 17 J/cm^2 respectively, and 5.3×10^{-2} and 8.5×10^{-2} for the silicone hydrogel at 0.5 J/cm^2 and 0.8 J/cm^2. Refractive index mechanism for these low scattering loss DLIP gratings can be attributed to additional cross-linking and local densification. These refractive index change values were similar to those reported by using the ULI technique but with an improvement of the processing yield of more than two orders of magnitude.

Acknowledgements

D. Sola thanks the PIT2 program of the University of Murcia (Spain) for the financial support of his contract. The international mobility program for abroad stays “José Castillejo” from the ministry of culture MECD under the grant CAS17/00177 is also acknowledged. This work was also supported by the European Research Council Advanced Grant ERC-2013-AdG-339228 (SEECAT), Secretaría de Estado e Investigación, Desarrollo e Innovación-SEIDI (FIS2016-76163-R), Fundación Séneca-Agencia de Ciencia y Tecnología de la Región de Murcia (19897/GERM/15), European Regional Development Fund (EU-FEDER). The work of S. Alamri has been supported by the European Union’s Horizon 2020 research and innovation programme under the Marie Skłodowska-Curie grant agreement No. 675063. The work of A.F. Lasagni is also supported by the German Research Foundation (DFG) under Excellence Initiative program by the German federal and state governments to promote top-level research at German universities.

References

[1] M.B. McDonald, R. Beuerman, W. Folzoni, L. Rivera, H.E. Kaufman, Refractive surgery with the excimer laser, Am. J. Ophthalmol. 103 (1987) 469.
[2] C.R. Munnerlyn, S.J. Koons, J. Marshall, Photorefractive keratectomy: a technique for laser refractive surgery, J. Cataract Refract. Surg. 14 (1988) 46–52.
[3] I.G. Pallikaris, M.E. Papatzanaki, E.Z. Stathi, O. Frenschock, A. Georgiadis, Laser in situ keratomileusis, Lasers Surg. Med. 10 (1990) 463–468.
[4] K. Nakamura, D. Kurosaka, H. Bissen-Miyajima, K. Tsubota, Intact corneal epithelium is essential for the prevention of stromal haze after laser assisted in situ keratomileusis, Br. J. Ophthalmol. 85 (2001) 209–213.
[5] M.V. Netto, R.R. Mohan, R. Jr, A.E. Ambrósio, J.D. Hutcheon, S.E. Wilson Zieske, Wound healing in the cornea: a review of refractive surgery complications and new prospects for therapy, Cornea 24 (2005) 509–522.
[6] R. Ambrósio, T. Tervo, S.E. Wilson, LASIK-associated dry eye and neurotrophic epitheliopathy: pathophysiology and strategies for prevention and treatment, J. Refract. Surg. 24 (2008) 396–407.
[7] H. Misawa, S. Juodkazis, 3D Laser Microfabrication, Wiley, 2006.
[8] K.M. Davis, K. Miura, N. Sugimoto, K. Hirao, Writing waveguides in glass with a femtosecond laser, Opt. Lett. 21 (1996) 1729–1731.
[9] S. Nolte, M. Will, J. Burghoff, A. Tuennermann, Femtosecond waveguide writing: a new avenue to three-dimensional integrated optics, Appl. Phys. A 77 (2003) 109–111.
[10] R.R. Gattas, E. Mazur, Femtosecond laser micromachining in transparent materials, Nat. Photon. 2 (2008) 219–225.
[11] D. Sola, A. Escartín, R. Cases, J.I. Peña, Crystal growth induced by Nd:YAG laser irradiation in patterning glass ceramic substrates with dots, Opt. Mater. 33 (2011) 728–734.
[12] D. Sola, J. Martinez de Mendibil, J.R. Vazquez de Aldana, G. Lifante, R. Balda, A.H. de Aza, P. Pena, J. Fernandez, Stress-induced buried waveguides in the $0.8CaSiO_3$-$0.2Ca_3(PO_4)_2$ eutectic glass doped with Nd^{3+} ions, Appl. Surf. Sci. 278 (2013) 289–294.
[13] F. Chen, J.R. Vazquez de Aldana, Optical waveguides in crystalline dielectric materials produced by femtosecond-laser micromachining, Laser Photon. Rev. 8 (2014) 251–275.

[14] D. Choudhury, J.R. Macdonald, A.K. Kar, Ultrafast laser inscription: perspectives on future integrated applications, Photon. Rev 8 (2014) 827–846.
[15] J. Martinez de Mendivil, D. Sola, J.R. Vazquez de Aldana, G. Lifante, A.H. de Aza, P. Pena, J.I. Peña, Ultrafast direct laser writing of cladding waveguides in the $0.8CaSiO_3$-$0.2Ca_3(PO_4)_2$ eutectic glass doped with Nd^{3+} ions, J. Appl. Phys. 117 (2015) 043104-1/5.
[16] L. Ding, R. Blackwell, J.F. Künzler, W.H. Knox, Large refractive index change in silicone-based and non-silicone-based hydrogel polymers induced by femtosecond laser micro-machining, Opt. Exp. 14 (2006) 11901–11909.
[17] L. Ding, D. Jani, J. Linhardt, J.F. Künzler, S. Pawar, G. Labenski, T. Smith, W.H. Knox, Large enhancement of femtosecond laser micromachining speed in dye-doped hydrogel polymers, Opt. Exp. 16 (2008) 21914–21921.
[18] L. Ding, D. Jani, J. Linhardt, J.F. Künzler, S. Pawar, G. Labenski, T. Smith, W.H. Knox, Optimization of femtosecond laser micromachining in hydrogel polymers, J. Opt. Soc. Am. 26 (2009) 1679–1687.
[19] L. Ding, W.H. Knox, J. Bühren, L.J. Nagy, K.R. Huxlin, Intratissue refractive index shaping (IRIS) of the cornea and lens using a low-pulse-energy femtosecond laser oscillator, Invest. Ophthalmol. Vis. Sci. 49 (2008) 5332–5339.
[20] L.J. Nagy, L. Ding, L. Xu, W.H. Knox, K.R. Huxlin, Potentiation of femtosecond laser intratissue refractive index shaping (IRIS) in the living cornea with sodium fluorescein, Invest. Ophthalmol. Vis. Sci. 51 (2010) 850–856.
[21] L. Xu, W.H. Knox, M. DeMagistris, N. Wang, K.R. Huxlin, Noninvasive intratissue refractive index shaping (IRIS) of the cornea with blue femtosecond laser light, Invest. Ophthalmol. Vis. Sci. 52 (2011) 8148–8155.
[22] D.E. Savage, D.R. Brooks, M. DeMagistris, L. Xu, S. MacRae, J.D. Ellis, W.H. Knox, K.R. Huxlin, First demonstration of ocular refractive change using blue-IRIS in live cats, Invest. Ophthalmol. Vis. Sci. 55 (2014) 4603–4612.
[23] K.T. Wozniak, S.M. Gearhart, D.E. Savage, J.D. Ellis, W.H. Knox, K.R. Huxlin, Comparable change in stromal refractive index of cat and human corneas following blue-IRIS, J. Biomed. Opt. 22 (2017) 055007.
[24] F. Yu, P. Li, H. Shen, S. Mathur, C.M. Lehr, U. Bakowsky, F. Mücklich, Laser interference lithography as a new and efficient technique for micropatterning of biopolymer surface, Biomaterials 26 (2005) 2307–2312.
[25] F.J. Rodríguez, C. Sánchez, B. Villacampa, R. Alcalá, R. Cases, M. Millaruelo, L. Oriol, Surface relief gratings induced by a nanosecond pulse in a liquid-crystalline azo-polymethacrylate, Appl. Phys. Lett. 87 (201914) (2005) 1–3.
[26] O.T. Picot, R. Alcalá, C. Sánchez, M. Dai, N.F. Hughes-Brittain, D.J. Broer, T. Peijs, C.W.M. Bastiaansen, Manufacturing of surface relief structures in moving substrates using photoembossing and pulsed-interference holography, Macromol. Mater. Eng. 298 (2013) 33–37.
[27] L. Müller-Meskamp, Y.H. Kim, T. Roch, S. Hofmann, R. Scholz, S. Eckardt, K. Leo, A.F. Lasagni, Efficiency enhancement of organic solar cells by fabricating periodic surface textures using direct laser interference patterning, Adv. Mater. 24 (2012) 906–910.
[28] D. Langheinrich, E. Yslas, M. Broglia, V. Rivarola, D. Acevedo, A.F. Lasagni, Control of cell growth direction by direct fabrication of periodic micro- and submicrometer arrays on polymers, J. Polym. Sci. B: Polym. Phys. 50 (2012) 415–422.
[29] M. Bieda, M. Siebold, A.F. Lasagni, Fabrication of sub-micron surface structures on copper, stainless steel and titanium using picosecond laser interference patterning, Appl. Surf. Sci. 387 (2016) 175–182.
[30] R. Estevam-Alves, D. Günther, S. Dani, S. Eckhardt, T. Roch, C.R. Mendonca, I.N. Cestari, A.F. Lasagni, UV Direct Laser Interference Patterning of polyurethane substrates as tool for tuning its surface wettability, Appl. Surf. Sci. 374 (2016) 222–228.
[31] V. Lang, T. Roch, A.F. Lasagni, High-speed surface structuring of polycarbonate using direct laser interference patterning: toward 1 m^2 min^{-1} fabrication speed barrier, Adv. Eng. Mater. 18 (2016) 1342–1348.
[32] S. Alamri, A.F. Lasagni, Development of a general model for direct laser interference patterning of polymers, Opt. Exp. 25 (2017) 9603–9616.
[33] S. Alamri, A.I. Aguilar-Morales, A.F. Lasagni, Controlling the wettability of polycarbonate substrates by producing hierarchical structures using direct laser interference patterning, Eur. Polym. J. 99 (2018) 27–37.
[34] D. Sola, C. Lavieja, A. Orera, M.J. Clemente, Direct laser interference patterning of ophthalmic polydimethylsiloxane (PDMS) polymers, Opt. Lasers Eng. 106 (2018) 139–146.
[35] R. Srinivasan, B. Braren, Ultraviolet laser ablation of organic polymers, Chem. Rev. 89 (1989) 1303–1316.
[36] R. Srinivasan, B. Braren, K.G. Casey, Nature of "incubation pulses" in the ultraviolet laser ablation of polymethyl methacrylate, J. Appl. Phys. 68 (1990) 1842.
[37] F. Beinhorn, J. Ihlemann, K. Luther, J. Troe, Micro-lens arrays generated by UV laser irradiation of doped PMMA, Appl. Phys. A 68 (1999) 709–713.
[38] T. Roch, F. Klein, K. Guenther, A. Roch, T. Mühl, A. Lasagni, Laser interference induced nanocrystallized surface swellings of amorphous carbon for advanced micro tribology, Mat. Res. Expr. 1 (2014) 035042.
[39] D. Sola, L. Grima, Laser machining and in vitro assessment of wollastonite-tricalcium phosphate eutectic glasses and glass-ceramics, Materials 11 (2018) 125.
[40] D. Sola, J.I. Peña, Study of the wavelength dependence in laser ablation of advanced ceramics and glass-ceramic materials in the nanosecond range, Materials 6 (2013) 5302–5313.
[41] D. Sola, J.I. Peña, Laser machining of Al_2O_3–ZrO_2 ($3\%Y_2O_3$) eutectic composite, J. Eur. Ceram. Soc. 32 (2012) 807–814.
[42] N. Bityurin, B.S. Luk'yanchuk, M.H. Hong, T.C. Chong, Models for laser ablation of polymers, Chem. Rev. 103 (2003) 519–552.
[43] P. Taddei, F. Balducci, R. Simoni, P. Monti, Raman, IR and thermal study of a new highly biocompatible phosphorylcholine-based contact lens, J. Mol. Struct. 744–747 (2005) 507–514.
[44] A. Bertoluzza, P. Monti, J.V. Garcia-Ramos, R. Simoni, R. Caramazza, A. Calzavara, Applications of Raman spectroscopy to the ophthalmological field: Raman spectra of soft contact lenses made of poly-2-hydroxyethylmethacrylate (PHEMA), J. Mol. Struct. 143 (1986) 469–472.
[45] Y. Sekine, T. Ikeda-Fukazawa, Structural changes of water in a hydrogel during dehydration, J. Chem. Phys. 130 (2009) 034501.
[46] L. Ding, L.G. Cancado, L. Novotny, W.H. Knox, N. Anderson, D. Jani, J. Linhardt, R.I. Blackwell, J.F. Künzler, Micro-Raman spectroscopy of refractive index microstructures in silicone-based hydrogel polymers created by high-repetition-rate femtosecond laser micromachining, J. Opt. Soc. Am. B 26 (2009) 595–602.
[47] P.J. Scully, D. Jones, D.A. Jaroszynski, Femtosecond laser irradiation of polymethylmethacrylate for refractive index gratings, J. Opt. A: Pure Appl. Opt. 5 (2003) S92–S96.
[48] H. Mochizuki, W. Watanabe, Y. Ozeki, K. Itoh, K. Matsuda, S. Hirono, Fabrication of diffractive optical elements inside polymers by femtosecond laser irradiation, Thin Solid Films 518 (2009) 714–718.
[49] A. Baum, P.J. Scully, W. Perrie, D. Liu, V. Lucarini, Mechanisms of femtosecond laser-induced refractive index modification of poly(methyl methacrylate), Jo. Opt. Soc. Am. B 27 (2010) 107–111.